

# Spectro-polarimetry of 4U 1957+115 with IXPE: Effects of spin and returning radiation on polarised emission of black hole in thermal state

Ankur Kushwaha<sup>1,2\*</sup>, Kiran M. Jayasurya<sup>1</sup>, Anuj Nandi<sup>1</sup>

<sup>1</sup>Space Astronomy Group, ISITE Campus, U. R. Rao Satellite Centre, Outer Ring Road, Marathahalli, Bangalore, 560037, India

<sup>2</sup>Department of Physics, Indian Institute of Science, Bangalore, 560012, India

Accepted XXX. Received YYY; in original form ZZZ

## ABSTRACT

We present a comprehensive spectro-polarimetric study of persistent Black hole X-ray binary 4U 1957+115 with *IXPE* and *NICER* observations. The source is observed in disk dominated thermal state with disk temperature,  $kT_{in} \approx 1.4$  keV. The emission during thermal state from the source is found to be moderately polarized and *IXPE* measures a degree of polarization (PD) =  $1.95 \pm 0.37\%$  ( $> 4.79\sigma$ ) along with a polarization angle (PA) =  $-42.78^\circ \pm 5.41^\circ$  in the energy range of 2 – 8 keV. PD is found to be an increasing function of energy, whereas PA indicates switching within the energy range which could be due to high inclination and the returning radiation within the system. Simultaneous energy spectra (0.6 – 10 keV) from *NICER* are modelled to study the spectral properties. Furthermore, the spin parameter of the black hole is estimated with spectro-polarimetric data as  $a_* = 0.988 \pm 0.001$  ( $1\sigma$ ), which is corroborated by *NICER* observations. Finally, we discuss the implications of our findings.

**Key words:** accretion, accretion disks – polarization – techniques: polarimetric – black hole physics – radiation: dynamics – X-ray: binaries – stars: individual (4U 1957+115)

## 1 INTRODUCTION

The X-ray polarimeter experiments are now detecting and investigating the polarimetric properties of bright galactic and extra-galactic X-ray objects. The Black hole X-ray binaries (BH-XRBs) are among the suitable candidates for X-ray polarimetric studies as they are bright and are predicted to emit polarised radiation (Rees 1975; Lightman & Shapiro 1975, 1976; Stark & Connors 1977; Connors & Stark 1977).

The polarimetric measurements are combined with simultaneous spectroscopic data for holistic approach to understand the emission processes in the vicinity of black hole. The spectro-polarimetric studies are also effective in probing the environment and accretion disk structure, which is formed surrounding the black hole with the matter accreted from the companion star. The Keplerian accretion disk is the main source of multi-coloured thermal radiation (Shakura & Sunyaev 1973; Novikov & Thorne 1973), while a Comptonizing medium is believed as the origin of the non-thermal component (Titarchuk 1994; Chakrabarti & Titarchuk 1995), typically present, in the spectra of different spectral states of BH-XRBs (Homan & Belloni 2005; Remillard & McClintock 2006; Nandi et al. 2012; Baby et al. 2020; Kushwaha et al. 2021, and references therein).

In recent years, the Imaging X-ray Polarimetry Explorer (*IXPE*; Weisskopf et al. (2022)) has provided high quality long exposure observations of a few persistent and transient BH-XRBs during different spectral states. The spectro-polarimetric studies have been reported for Cyg X-1 (Krawczynski et al. 2022), Cyg X-3 (Vedina et al. 2023), 4U 1630–47 (Kushwaha et al. 2023; Rawat et al.

2023; Ratheesh et al. 2023; Rodriguez Cavero et al. 2023), LMC X-1 (Podgorny et al. 2023) and LMC X-3 (Majumder et al. 2023; Svoboda et al. 2023). Polarimetric properties of Cyg X-1 in low/hard state (LHS) and of 4U 1630–47 in high/soft state (HSS) as well as in steep power law state (SPL) are reported to be inconsistent with the existing models (Dovčiak et al. 2008; Schnittman & Krolik 2009; Taverna et al. 2020). These sources exhibit higher degree of polarization (PD) with unexpected energy dependence of polarization angle (PA), while the polarimetric observables of LMC X-1 and LMC X-3 in HSS are inline with the ones anticipated from the systems.

Moreover, the X-ray emission, during HSS, of BH-XRBs deeply affected by the spin of the BH and returning radiation that causes depolarization which results into reduction of net PD and rotation of PA (Connors et al. 1980; Schnittman & Krolik 2009). Hence, a BH-XRB with rapidly spinning BH is expected to exhibit lower PD than that of a system with a slow spinning BH (larger inner disk radius). In order to verify these effects, we conduct a spectro-polarimetric study of 4U 1957+115 combining polarimetric data of *IXPE* observations with simultaneous spectral data of *NICER*.

4U 1957+115 is a persistent low mass X-ray binary system harbouring a black hole (Margon et al. 1978; Thorstensen 1987; Hakala et al. 1999). It is located in galactic halo (away from galactic plane) and has a low absorption column density of  $N_H \sim 0.1 \times 10^{22} \text{ cm}^{-2}$  (Yaqoob et al. 1993; Nowak & Wilms 1999). The estimation of mass ( $M_{BH}$ ), distance ( $D$ ) and inclination ( $i$ ) of the system have been attempted in multiple studies based on optical and X-ray, but are not very definitive. The best estimation of these parameters are  $M_{BH} < 10 M_\odot$ ,  $D \leq 30$  kpc and high inclination of  $i \sim 70^\circ - 75^\circ$  (Hakala et al. 1999; Bayless et al. 2011; Mason et al. 2012; Gomez et al. 2015; Maccarone et al. 2020; Sharma et al. 2021; Barillier et al. 2023). X-ray

\* E-mail: ankursh@ursc.gov.in

**Table 1.** Log of *NICER* and *IXPE* observations of 4U 1957+115 considered in the analysis. From left to right, (1) observation identifier; (2) observation ID; (3) MJD of observation; (4) exposure time.

Obs Name	ObsID	Start MJD	Exposure (ksec)
NICER			
N1	6100400102	60078	~2.9
N2	6100400103	60079	~4.6
N3	6100400104	60080	~8.0
N4	6100400105	60081	~5.1
N5	6100400106	60082	~11.7
N6	6100400107	60083	~3.9
N7	6100400108	60084	~5.0
N8	6100400109	60085	~8.2
N9	6100400110	60086	~2.7
N10	6100400111	60087	~4.2
N11	6100400112	60088	~2.8
IXPE			
X1	02006601	59814	~572 (~ 15 days)

observations also suggest that the source hosts a rapidly rotating BH (Nowak & Wilms 1999; Nowak et al. 2008, 2012; Sharma et al. 2021; Draghis et al. 2023) In a recent study, with *NICER* and *NuSTAR* the spectral fits result spin parameter:  $a_* = 0.9961 \pm 0.0003$  (Barillier et al. 2023).

4U 1957+115, till date, has remained in disk dominated HSS since its detection in 1973 (Yaqoob et al. 1993; Nowak & Wilms 1999; Maitra et al. 2014; Nowak et al. 2012; Maccarone et al. 2020; Mudambi et al. 2022) and emits persistent flux in X-rays which is comparable to that of LMC X-1 and LMC X-3 (Bhuvana et al. 2022). Moreover, detailed polarization measurement during HSS of 4U 1957+115, to the best of our knowledge, has not been reported so far.

In this work, we focus on the spectro-polarimetric study of 4U 1957+115. We make use of *IXPE* (2 – 8 keV) and *NICER* (0.6 – 10 keV) data to study simultaneous polarimetric and spectral properties of 4U 1957+115. The spin of BH is also estimated with spectral and spectro-polarimetric modelling.

In §2, we provide details of the observations and the steps for data reduction. The polarimetric properties and spectro-polarimetric data modelling using both *NICER* as well as *IXPE* are presented in §3. Finally, we discuss the results and conclude in §4.

## 2 OBSERVATIONS AND DATA REDUCTION

### 2.1 IXPE

*IXPE* is an imaging polarimeter (Weisskopf et al. 2022) consisting of three detector units (DUs) which are polarization sensitive in the 2 – 8 keV energy range. It observed 4U 1957+115 from 12 May, 2023 (MJD 60076) to 26 May, 2023 (MJD 60090) for ~ 572 ksec (Table 1). The Level-2 data of the observation are reduced and analysed with *IXPEOBSIMv30.0.0* (Baldini et al. 2022) following the procedure of Farinelli et al. (2023). Further, *XPSELECT* task is used to extract the source and background event lists. The source is considered within a circular region of 80'' and the background region as an annular region with inner & outer radii of 180'' & 240'', respectively. Subsequently, the *XPBIN* task is used to generate the polarization cubes using the *PCUBE* algorithm. The Stokes I, Q and U spectra

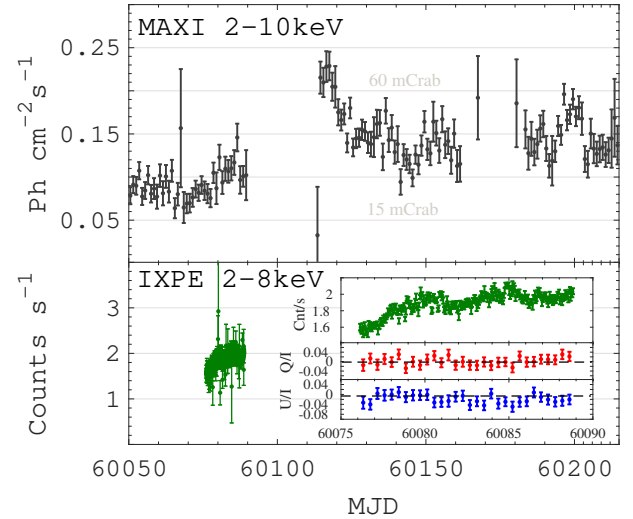


**Figure 1.** Top to bottom: The light curve of 4U 1957+115 obtained from *MAXI* (purple; 1 day averaged) and all three DUs of *IXPE* (green; 2 ksec bin time). The inset in the bottom panel shows *IXPE* light curve (4 ksec bin time) along with the temporal variation of normalized Stokes parameters *Q/I* and *U/I* (~36 ksec bin time). The corresponding energy ranges of light curves are also mentioned in each panel. See the text for details.

of source and background are generated with the *PHA1*, *PHA1Q* and *PHA1U* algorithms. The light curves in 2 – 8 keV energy band for the different DUs are generated with the *XSELECT* task of *HEASOFT* v6.31.1 and added using the *lcmath* task to get a combined light curve (see bottom panel of Figure 1).

### 2.2 NICER

*NICER* observed the source from 12 May, 2023 (MJD 60076) to 24 May, 2023 (MJD 60088) which overlaps with *IXPE* observations (see Table 1 and Figure 1). We make use of eleven observations of during this interval are analyzed for this work. The *NICERDASv10* software distributed with *HEASOFT* v6.31.1 is used along with the latest *CALDB* to reduce the data from the observations. The *nicer12* task is used to perform standard calibration and screening to generate cleaned event lists. The source and background spectra along with the responses are generated in the 0.5 – 12 keV energy band using the *nicer13-spect* task. The spectra are rebinned to have a minimum of 25 counts per energy bin for spectral modelling.

## 3 MODELLING AND RESULTS

### 3.1 Polarimetric Properties

*IXPE* observes 4U 1957+115 for ~ 572 ksec which spanned over ~ 15 days (see Table 1). The *IXPE* light curve is shown in Figure 1. The source emanates a persistent flux during the exposure with slight increase in count rate. The averaged count rate (from 3 DUs) increased from about 1.6 cts/s to 2 cts/s at the start and end of the observation, respectively. The temporal variation of the polarization observables: normalized Stokes parameters (*Q/I* & *U/I*) are also shown in the Figure 1 (Inset of bottom panel). We note that the variability is within statistical limits. In order to investigate polarimetric properties for the first time from this source, we adopt the methodology of Kushwaha et al. (2023); Chatterjee et al. (2023); Jayasurya et al. (2023). Firstly,

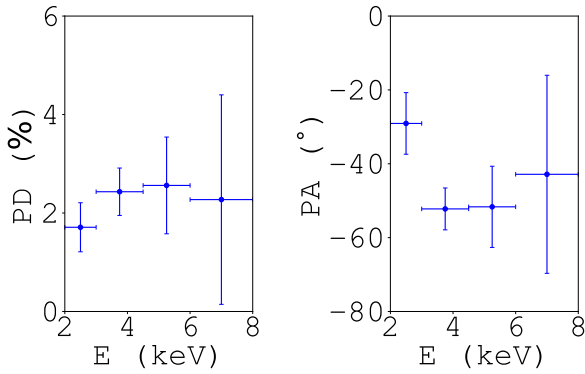


**Figure 2.** Polarization degree and associated polarization angle measured from 4U 1957+115 with *IXPE* observations. See the text for details.

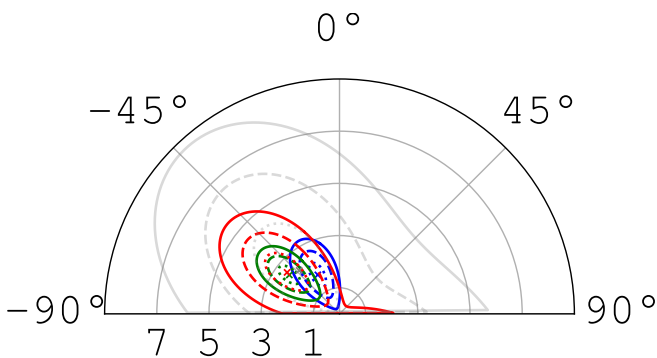


**Figure 3.** The confidence contours ( $1\sigma$  [dotted],  $2\sigma$  [dashed] and  $3\sigma$  [solid]) of PA and PD obtained with PCUBE in 2 – 3 (blue), 3 – 4.5 (green), 4.5 – 6 (red) and 6 – 8 keV (grey) energy bins. The grid shows PA ( $^\circ$ ) on radial lines and PD (%) as concentric rings. See the text for details.

the model-independent PCUBE algorithm (Kislat et al. 2015) is used to determine the normalized Stokes parameters ( $Q/I$  &  $U/I$ ) and polarization degree (PD) and polarization angle (PA) are derived in the 2 – 3 keV, 3 – 4.5 keV, 4.5 – 6 keV, 6 – 8 keV and in the total 2 – 8 keV energy ranges. The resulting parameters along with corresponding MDP and statistical significance are provided in Table 2. The polarization measurements are above the MDP and significant upto 4.5 keV energy range. The measurements in higher energy range are less reliable. Alternatively, we also derived PD in 2 – 4 and 4 – 8 keV energy ranges as  $1.58 \pm 0.36\%$  ( $> 3.75\sigma$ ; 1.10% MDP<sub>99</sub>) and  $3.26 \pm 0.76\%$  ( $> 3.67\sigma$ ; 2.33% MDP<sub>99</sub>), respectively. These measurements evidently suggest an increasing nature of PD with energy. PA is noted to be rapidly declining from  $\sim -30^\circ$  to  $\sim -50^\circ$ . The variation of PD and PA with energy is shown in Figure 2.

The measured PD and PA in different energy ranges spanning 2 – 8 keV are also plotted with error contours (see Figure 3). We note a PD =  $1.95\% \pm 0.37\%$  in 2 – 8 keV energy band with all the event data from three DUs combined. The PA in the same energy band is found to be  $-42.78^\circ \pm 5.41^\circ$ .

### 3.2 Spectral Modelling

We consider 0.6 – 10.0 keV range of *NICER* data to model the spectra of all the observations (see Table 1) of 4U 1957 + 115. Firstly, we fit

a phenomenological model `Tbabs*diskbb` on the set of spectra. All the spectra are fitted at once without tying the parameters. The model results in good fits and residual does not suggest any requirement of a power-law towards the high energy in the spectra. It indicates that the source is in a steady disk dominated state during multiple observations of *NICER*. The fits give an average disk temperature of  $kT_{in} \approx 1.4 \pm 0.01$  keV. The combined fit statistics for 11 spectra results into a  $\chi^2_{red}$  ( $\chi^2/dof$ ) = 0.93. The hydrogen column density  $N_H$  is estimated to be  $\approx 0.85 \times 10^{22}$  atoms  $\text{cm}^{-2}$  from the group spectral fits. The estimation of  $N_H$  is consistent with previous estimates from spectral studies (Yaqoob et al. 1993; Nowak & Wilms 1999; Maitra et al. 2014; Nowak et al. 2012; Maccarone et al. 2020; Mudambi et al. 2022; Barillier et al. 2023). The overall fit of obs. N5 is shown in Figure 4.

### 3.3 Spin Estimation with Continuum Fitting (CF) Method

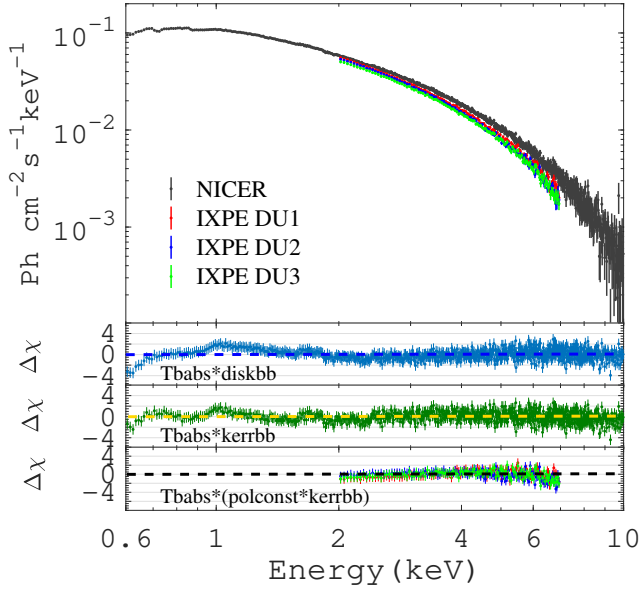
In § 3.2, it is shown that the source exhibits a steady disk dominated soft state during *NICER* observations. Further, the CF method is employed and only large exposure spectra (Obs. N3, N5 and N8) are modelled with relativistic model to estimate the spin parameter of BH. For relativistic modelling of spectra, we follow Kushwaha et al. (2021) and replace `diskbb` with `kerrbb` in our previous model mentioned in § 3.2. Hence, we fit all spectra with `Tbabs*kerrbb`. The model results into reasonably acceptable fits. We, once again, introduce a power-law component `simpl` to check if there is any signature of non-thermal component of corona present in the spectra. We do not observe any improvement in overall fit and notice unacceptable values of parameters in `simpl` component. Therefore, we continue to fit the spectra with our initial `kerrbb` model, which is a relativistic thin accretion disk model and includes self-irradiation along with limb-darkening effects. We switch off limb-darkening and apply zero torque condition at the inner boundary of the disk. Moreover, model is provided with best estimations of distance to source ( $D$ ), mass of the black hole ( $M_{BH}$ ) in the binary system and inclination of the binary plane ( $i$ ) based on the published works (see § 1 and references therein). Hence, we fix the distance at  $D = 16$  kpc, the inclination at  $i = 75^\circ$ , black hole mass at  $M = 8M_\odot$ . The spectral hardening factor ( $f$ ) is fixed to a fiducial value of 1.6 (Shimura & Takahara 1995). The other two parameters of `kerrbb` namely accretion rate ( $\dot{M}$ ) and spin parameter ( $a_*$ ) are allowed to vary freely. For obs. N5, overall fit estimates  $N_H = 0.11 \pm 0.01 \times 10^{22}$  atoms  $\text{cm}^{-2}$ ,  $a_* = 0.994 \pm 0.002$  and  $\dot{M} = 0.13 \pm 0.01 \times 10^{18}$   $\text{g s}^{-1}$  with  $\chi^2_{red}$  ( $\chi^2/dof$ ) = 0.93(792.5.65/850). We highlight the fact that estimation of spin parameter is highly dependent on  $D$ ,  $M$  and  $i$ . Further, similar fit procedure is applied to rest of the observations to estimate the spin. We notice a consistent value of spin parameter from all the selected observation from HSS of 4U 1957 + 115. The best fitting model unfolded against the spectral data for obs. N5 is shown in Figure 4.

### 3.4 Spectro-polarimetric Analysis

Subsequently, we also perform model-dependent analysis by fitting *IXPE* Stokes I, Q and U spectra in XSPEC. We make use of the relativistic model as described in § 3.3 and introduce the multiplicative component `polpow` which has PA and PD as function of energy. The component defines  $PD(E) = A_{norm} \times E^{-A_{index}}$  and  $PA(E) = ps_{inorm} \times E^{-ps_{index}}$ . The `polpow` is chosen for polarimetric component based on the results of PCUBE algorithm that shows that PD and PA are energy dependent. Hence, the model `Tbabs(polpow*kerrbb)`

**Table 2.** Polarization parameters obtained using the PCUBE algorithm (for all 3 DUs combined) in different energy bands. The uncertainties are reported at  $1\sigma$  level. The symbol  $\dagger$  denotes value below zero.

Parameter	2 – 3 keV	3 – 4.5 keV	4.5 – 6 keV	6 – 8 keV	2 – 8 keV
Q/I (%)	$0.9 \pm 0.5$	$-0.61 \pm 0.48$	$-0.59 \pm 0.98$	$0.17 \pm 2.13$	$0.15 \pm 0.37$
U/I (%)	$-1.45 \pm 0.5$	$-2.36 \pm 0.48$	$-2.49 \pm 0.98$	$-2.27 \pm 2.13$	$-1.94 \pm 0.37$
PD (%)	$1.71 \pm 0.5$	$2.43 \pm 0.48$	$2.56 \pm 0.98$	$2.27 \pm 2.13$	$1.95 \pm 0.37$
PA ( $^\circ$ )	$-29.08 \pm 8.34$	$-52.22 \pm 5.67$	$-51.66 \pm 10.99$	$-42.85 \pm 26.82$	$-42.78 \pm 5.41$
MDP <sub>99</sub> (%)	1.51	1.46	2.98	6.45	1.12
Signif.( $\sigma$ )	2.78	4.54	1.83	$-\dagger$	4.79

**Figure 4.** 4U 1957+115 spectra (unfolded) obtained from *NICER* observations. N5 is shown along with *IXPE* (DU1, 2 and 3) in top panel. Bottom panels show the residuals (in units of  $\sigma$ ) corresponding to each model considered in this work. See the text for details.

is applied to fit three Stokes spectra from all the DUs of *IXPE* in XSPEC. Only parameters of *polpow* component and  $a_*$ ,  $\dot{M}$  of *kerrbb* are kept free for the fit. All other parameters are frozen to average values obtained from *NICER* spectral fits (see §3.2). The fit procedure results into an acceptable  $\chi^2_{red}(\chi^2/dof) = 0.93(1103.6/1108)$  for combined nine spectra (I, Q & U for 3 DUs). Moreover, we replace *polpow* with *polconst* to verify the polarization measurements in overall 2 – 8 keV energy range as well with assuming no energy dependence. The best fit values are provided in the Table 3.

The overall fit and modelled spectra are shown in Figure 4. Furthermore, the model-dependent polarization results are compared with those obtained in model-independent method by integrating PD(E) and PA(E) using *polpow* parameters in the 2 – 8 keV energy range. PD and PA are estimated to be 2.6% and  $\sim -52^\circ$ , respectively. We notice that parameters of *polpow* have large uncertainties and poor constraints. The *polconst* component parameters result  $1.8\% \pm 0.2\%$  and  $-43^\circ \pm 5.2^\circ$  for PD and PA respectively. We notice measurements of PA and PD obtained from XSPEC differ marginally from results of PCUBE algorithm. We outline that the spin parameters values resulting from *IXPE* (see Table 3) polarimetric fits are inline with the values obtained by *NICER* spectral fits (see §3.2).

**Table 3.** The best fit spectral parameters from *IXPE* observations of 4U 1957+115 with spectro-polarimetric model. From left to right are, (1) model components; (2) parameters values of components with *polconst*; (3) with *polpow*. The parameters that are fixed during the fits are denoted with <sup>fixed</sup>.

Components	Model	
	Tbabs* <i>polconst</i> * <i>kerrbb</i>	Tbabs* <i>polpow</i> * <i>kerrbb</i>
$A_{norm}(\times 10^{-2})$	$1.8 \pm 0.2$	$0.54 \pm 0.3$
$A_{index}$	-	$-1.08 \pm 0.3$
$ps_{inorm}$	$-43.1 \pm 5.2$	$-14.4 \pm 6.3$
$ps_{index}$	-	$-0.87 \pm 0.01$
$N_H(\times 10^{22} \text{ cm}^{-2})$	$0.11^{\text{fixed}}$	$0.11^{\text{fixed}}$
$a_*$	$0.988 \pm 0.001$	$0.983 \pm 0.003$
$\dot{M}(\times 10^{18} \text{ g s}^{-1})$	$0.13 \pm 0.01$	$0.15 \pm 0.02$
$\chi^2_{red}(\chi^2/dof)$	0.93 (1013.54/1109)	0.91 (1013.6/1108)

## 4 DISCUSSION

In this letter, we report the measurements of X-ray polarization from a persistent low mass BH-XRB 4U 1957+115 by *IXPE* during HSS. The polarization properties are combined with simultaneous spectral modelling of *NICER* observations for spectro-polarimetric study of the source.

Our finding, based on spectro-polarimetric fits with constant polarization component model gives measurements of PD=  $1.8\% \pm 0.2\%$  and PA=  $-43^\circ \pm 5.2^\circ$  in 2 – 8 keV energy range. The model-independent approach using PCUBE algorithm estimates PD=  $1.95\% \pm 0.37\%$  and PA=  $-42.78^\circ \pm 5.41^\circ$ . These measurements are in good agreement. However, spectral modelling with inclusion of an energy-dependent component results into marginally higher values of polarization with PD $\sim 2.6\%$  and PA=  $-52^\circ$  in 2 – 8 keV energy range.

Moreover, we notice an increasing nature of PD with energy when PD is estimated in different energy ranges using *xpbin* tool (see Figure 2). Such energy dependence is previously observed in HSS of 4U 1630–47 (Kushwaha et al. 2023; Rawat et al. 2023; Ratheesh et al. 2023) and LMC-X3 (Majumder et al. 2023; Svoboda et al. 2023). We compare the PD with the same of LMC X-3 which is consistent with existing theoretical models. LMC X-3 and 4U 1957+115 have roughly similar high inclination angles but the former has a BH with lower spin than the later. Thermal disk emission from a low spin high inclination BH system is expected to show higher PD than the one with high spin high inclination. A slow spinning BH, where the inner disk radius is large, the polarization angle does not rotate much. For a high spin BH, where the inner disk radius is small, the polarization angle of the photons produced at the inner parts of the disk is much rotated, causing depolarization. Therefore, the net polarization is lower in the case of a higher BH spin (Mikusincova et al. 2023, and references therein). This can be related to the cases

of LMC X-3 and 4U 1957+115 as the observed PD is about 3% and 2%, respectively up to 5 keV. For a comparison above 5keV more *IXPE* observation are required as the polarimetric results suffer poor statistics near higher energies.

PD is also affected by returning radiation (Connors et al. 1980; Schnittman & Krolik 2009) and its albedo (Taverna et al. 2020; Mikusincova et al. 2023) on the accretion disk. The returning radiation have significant effect on polarization around high spin BH where the inner radius of disk is small which causes more returning radiation to scatter from the near side of the disk when compared to low spin BH. The returning radiation shows up as higher polarisation but in higher energies and may not be captured within *IXPE* energy range, but interestingly it also causes switching of PA within 2 – 8 keV from a BH thermal disk with appropriate albedo. Hence, a low spin BH is expected to have a roughly constant PA while a high spin BH will have a switching PA to lower values (Taverna et al. 2020; Mikusincova et al. 2023). We observe a rapidly declining PA from about  $-30^\circ$  to  $-50^\circ$  which could be an indication of switching PA in 4U 1957+115. Such switching is not present in the case of LMC X-3 which exhibits an anticipated constant PA of  $\sim -42^\circ$ .

We also highlight the fact that measurements of PA for 4U 1957+115 can not be related to orientation of system or disk plane as there is no radio activity detected from the source. We note that averaged PA measured in 2 – 8 keV of 4U 1957+115 is comparable to that of observed in case of LMC X-3.

Furthermore, spectro-polarimetric fit of *IXPE* data with relativistic model also constrains the BH spin parameter:  $a_* = 0.988 \pm 0.001$  ( $1\sigma$ ) and accretion rate:  $\dot{M} = (0.13 \pm 0.01) \times 10^{18} \text{ g s}^{-1}$ .

We compare the value of  $a_*$  with that obtained by applying CF method on *NICER* spectra which resulted  $a_* = 0.994 \pm 0.002$  ( $1\sigma$ ). The spin parameter estimated with two different approaches are in good agreement. The estimations are also in line with findings of Barillier et al. (2023) Here, we highlight the fact that estimation of spin parameter is highly dependent on  $i$ ,  $D$  and  $M$ .

To summarize, we report measurement of polarized emission from 4U 1957+115 during disk dominated high soft state. The observed degree of polarization and associated angle indicate the effects of high spin, high inclination and returning radiation within the system. The overall polarisation properties are consistent, at low energies, with expected from existing models. For definitive conclusion in higher energies longer exposure polarimetric observations are required.

## ACKNOWLEDGEMENTS

Authors thank GH, SAG; DD, PDMSA and Director, URSC for encouragement and continuous support to carry out this research. *IXPE*, *NICER* and *MAXI* teams are also thanked for providing data products and software tools for data analysis.

## DATA AVAILABILITY

Data used for this work are available at *HEASARC* website (<https://heasarc.gsfc.nasa.gov/docs/archive.html>) and *MAXI* website (<http://maxi.riken.jp/top/index.html>).

## REFERENCES

Baby B. E., Agrawal V. K., Ramadevi M. C., Katoch T., Antia H. M., Mandal S., Nandi A., 2020, *MNRAS*, 497, 1197  
Baldini L., et al., 2022, *SoftwareX*, 19, 101194

Barillier E., Grinberg V., Horn D., Nowak M. A., Remillard R. A., Steiner J. F., Walton D. J., Wilms J., 2023, *ApJ*, 944, 165  
Bayless A. J., Robinson E. L., Mason P. A., Robertson P., 2011, *ApJ*, 730, 43  
Bhuvana G. R., Radhika D., Nandi A., 2022, *Advances in Space Research*, 69, 483  
Chakrabarti S., Titarchuk L. G., 1995, *ApJ*, 455, 623  
Chatterjee R., Agrawal V. K., Jayasurya K. M., Katoch T., 2023, *MNRAS*, 521, L74  
Connors P. A., Stark R. F., 1977, *Nature*, 269, 128  
Connors P. A., Piran T., Stark R. F., 1980, *ApJ*, 235, 224  
Dovčiak M., Muleri F., Goosmann R. W., Karas V., Matt G., 2008, *MNRAS*, 391, 32  
Draghis P. A., Miller J. M., Zoghbi A., Reynolds M., Costantini E., Gallo L. C., Tomsick J. A., 2023, *ApJ*, 946, 19  
Farinelli R., et al., 2023, *MNRAS*, 519, 3681  
Gomez S., Mason P. A., Robinson E. L., 2015, *ApJ*, 809, 9  
Hakala P. J., Muhli P., Dubus G., 1999, *MNRAS*, 306, 701  
Homan J., Belloni T., 2005, *Ap&SS*, 300, 107  
Jayasurya K. M., Agrawal V. K., Chatterjee R., 2023, *MNRAS*, 525, 4657  
Kislat F., Clark B., Beilicke M., Krawczynski H., 2015, *Astroparticle Physics*, 68, 45  
Krawczynski H., et al., 2022, *Science*, 378, 650  
Kushwaha A., Agrawal V. K., Nandi A., 2021, *MNRAS*, 507, 2602  
Kushwaha A., Jayasurya K. M., Agrawal V. K., Nandi A., 2023, *MNRAS*, 524, L15  
Lightman A. P., Shapiro S. L., 1975, *ApJ*, 198, L73  
Lightman A. P., Shapiro S. L., 1976, *ApJ*, 203, 701  
Maccarone T. J., Osler A., Miller-Jones J. C. A., Atri P., Russell D. M., Meier D. L., McHardy I. M., Longa-Peña P. A., 2020, *MNRAS*, 498, L40  
Maitra D., Miller J. M., Reynolds M. T., Reis R., Nowak M., 2014, *ApJ*, 794, 85  
Majumder S., Kushwaha A., Das S., Nandi A., 2023, *arXiv e-prints*, p. arXiv:2309.06845  
Margon B., Thorstensen J. R., Bowyer S., 1978, *ApJ*, 221, 907  
Mason P. A., Robinson E. L., Bayless A. J., Hakala P. J., 2012, *AJ*, 144, 108  
Mikusincova R., Dovciak M., Bursa M., Lalla N. D., Matt G., Svoboda J., Taverna R., Zhang W., 2023, *MNRAS*, 519, 6138  
Mudambi S. P., Gudennavar S. B., Misra R., Bubbly S. G., 2022, *MNRAS*, 517, 4489  
Nandi A., Debnath D., Mandal S., Chakrabarti S. K., 2012, *A&A*, 542, A56  
Novikov I. D., Thorne K. S., 1973, in *Black Holes (Les Astres Occlus)*. pp 343–450  
Nowak M. A., Wilms J., 1999, *ApJ*, 522, 476  
Nowak M. A., Juett A., Homan J., Yao Y., Wilms J., Schulz N. S., Canizares C. R., 2008, *ApJ*, 689, 1199  
Nowak M. A., Wilms J., Pottschmidt K., Schulz N., Maitra D., Miller J., 2012, *ApJ*, 744, 107  
Podgorny J., et al., 2023, *arXiv e-prints*, p. arXiv:2303.12034  
Ratheesh A., et al., 2023, *arXiv e-prints*, p. arXiv:2304.12752  
Rawat D., Garg A., Méndez M., 2023, *ApJ*, 949, L43  
Rees M. J., 1975, *MNRAS*, 171, 457  
Remillard R. A., McClintock J. E., 2006, *ARA&A*, 44, 49  
Rodríguez Caverio N., et al., 2023, *arXiv e-prints*, p. arXiv:2305.10630  
Schnittman J. D., Krolik J. H., 2009, *ApJ*, 701, 1175  
Shakura N. I., Sunyaev R. A., 1973, *A&A*, 500, 33  
Sharma P., Sharma R., Jain C., Dewangan G. C., Dutta A., 2021, *Research in Astronomy and Astrophysics*, 21, 214  
Shimura T., Takahara F., 1995, *ApJ*, 445, 780  
Stark R. F., Connors P. A., 1977, *Nature*, 266, 429  
Svoboda J., et al., 2023, *arXiv e-prints*, p. arXiv:2309.10813  
Taverna R., Zhang W., Dovčiak M., Bianchi S., Bursa M., Karas V., Matt G., 2020, *MNRAS*, 493, 4960  
Thorstensen J. R., 1987, *ApJ*, 312, 739  
Titarchuk L., 1994, *ApJ*, 434, 570  
Veledina A., et al., 2023, *arXiv e-prints*, p. arXiv:2303.01174  
Weisskopf M. C., et al., 2022, *Journal of Astronomical Telescopes, Instruments, and Systems*, 8, 026002  
Yaqoob T., Ebisawa K., Mitsuda K., 1993, *MNRAS*, 264, 411

This paper has been typeset from a  $\text{\TeX}/\text{\LaTeX}$  file prepared by the author.